High-Energy Density Flow Battery Validation

Galen J. Suppes, Bryan D. Sawyer, and Michael J. Gordon
Dept. of Chemical Engineering, University of Missouri, Columbia, MO 65211

DOI 10.1002/aic.12390
Published online August 26, 2010 in Wiley Online Library (wileyonlinelibrary.com).

A zinc-alkaline flow cell was used to validate a new type of flow battery in which all reagents and products remain as solids on the electrodes. In every case, flow of electrolyte reduced overpotential losses when compared with operation without electrolyte flow. Large separation distances between the electrodes resulting from larger sections of separating tubing led to increased overpotential losses. A mass transfer mechanism is proposed that substantiates increasing overpotential with increasing electrode separation distances. Based on this mechanism, it was hypothesized that ion exchange packing would reduce the overpotential losses; this hypothesis was experimentally validated. © 2010 American Institute of Chemical Engineers *AIChE J,* 57: 1961–1967, 2011

Keywords: battery, flow, energy, packed-bed electrode, electrolyte

Introduction

Most commercial batteries rely on diffusion of ions between electrodes to complete the circuit in sandwich-type battery configurations. To maximize diffusion, the electrodes are packed closely together with polymer, cellulose, or fiberglass separators inhibiting the direct contact (short circuit) of counter electrodes. As a result, battery costs tend to be dominated by manufacturing and membrane costs that considerably exceed the cost of the active reagents.[1,2] This article describes the validation of a new type of flow battery that pumps electrolyte between reagents loaded in packed-bed electrodes separated by a permeable ion-exchange material.

The four basic components of a battery are as follows: (1) the anode in which electron-generating half-reactions occur, (2) the cathode in which electron-consuming reactions occur, (3) an electrically conductive path from the anode to the cathode that does not conduct ions, and (4) an ion-conductive electrolyte between electrodes that does not conduct electrons. Figure 1 illustrates how these basic components can manifest into either a sandwich configuration designed to maximize diffusive mass transfer or a flow battery configuration with convective mass transfer.

The ion transport in most commercial batteries relies on bulk diffusion, which has the advantage of no moving parts. To maximize diffusion, these sandwich configuration designs use thin membranes and relatively thin electrode layers, such as in spiral designs[3]; this introduces a variety of design constraints. For example, metallic lithium is not used in rechargeable batteries because the recharging of metallic lithium can lead to dendrite crystal growth that can traverse through the membrane separator and short circuit the battery. The standard approach to avoid dendrite growth is to use a graphite support for lithium ions in which the lithium exists in an intercalated state that has about 50 mV less potential than that is needed to form dendrite crystals. The maximum loading of the intercalated lithium is 1:6 (moles, lithium:carbon). The result is that active chemical reagents, like lithium, often tend to be a minor component in a battery with the major costs being directly or indirectly related to design constraints associated with the need for high separator areas and thin electrodes—both used to reduce diffusion overpotential.

The goal of this work is to validate a new type of flow battery that can be systematically used to reduce battery costs by reducing the use of separators and increasing the thicknesses of electrodes. The zinc-alkaline battery chemistry was used to test this new type of flow battery design; however, it is applicable to other chemistries as well.

Background

The term "flow battery"[4–7] traditionally refers to a class of batteries in which at least one reactant or product is not a

Correspondence concerning this article should be addressed to G. J. Suppes at suppesg@missouri.edu.

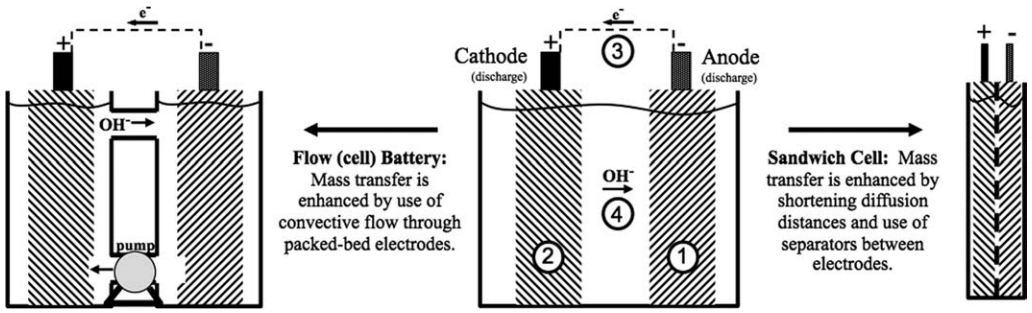

Figure 1. Schematic of a battery.

Illustration of components with four basic functions (1-anode, 2-cathode, 3-electron transport, 4-ion transport) and the transformation of these basic components into the sandwich cell for diffusive mass transfer and the flow cell for convective mass transfer.

solid phase on an electrode and the flow of electrolyte facilitates the transfer of that reactant/product to the electrodes. A distinguishing feature of the flow battery is that at least one substrate (or product) is stored externally to the electrode assemblies, typically in a tank of electrolyte. Flow batteries that have been extensively studied include those relying on soluble lead (in methanesulfonic acid),[8–10] soluble copper (as copper sulfate),[11] soluble zinc (in alkaline water or as zinc chloride),[7,12] chlorine as liquid $SOCl_2$,[13] chlorine gas,[14] and oxygen gas.[15]

The redox (reduction–oxidation)[16] cell is a type of flow battery in which all reagents/products are stored in the electrolyte. In the redox cell, the electrodes serve only as an electrochemical reactor; the power output scales with the electrodes, whereas the stored energy is independent of the electrodes. Redox flow batteries can be rapidly recharged by refilling the tank with fresh electrolyte.

Flow batteries have a few major advantages over traditional diffusion-based battery designs. For instance, higher power output is possible with the flow (reported to 500 mA/cm^2) of electrolyte when one of the reagents is stored in the electrolyte.[13] For these high-power output batteries, the flow of electrolyte also facilitates heat removal. Elimination or substantial reduction of membrane separators is another advantage of flow batteries.

The flow battery proposed in this work is different than the traditional flow batteries because all reagents and products reside as solids, which are part of the electrodes. Ionic intermediates flow through the electrolyte but do not accumulate. An advantage of having solid reagents is that the activity of the reagents remains nearly constant during use, whereas both the concentration and voltages from soluble reagents will decrease with use. Solid-substrate batteries also tend to have higher energy densities because of a more constant voltage output and the higher molar densities of pure solid reagents vs. solvated reagents.

In the proposed flow battery, as shown in Figure 2, a pump circulates electrolyte between stacked electrodes. The goal is to pump ions between the electrodes at mass transfer rates greater than that is possible with diffusion alone. The distances between electrodes in this design can be increased from microns to millimeters, and even up to centimeters. Zhang et al.[7] reported that dendrite growth is substantially absent when plating zinc in a flow battery. When dendrite growth is not inhibited by the flow or control of flow, the flow battery creates the opportunity to increase separation of distances between electrodes to the point where dendrite modes of failure can be substantially eliminated. In sandwich cell configurations, separation distances created by separators are typically less than 50 μm, and these short distances are easily traversed by dendrite crystal growth. The dendrite mode of failure would be much easier to control (e.g., with electrolyte flow or pulse charging) with separation distances of 1000 μm or more.

For small batteries, the diffusion-based architectures are superior because the cost of the circulating pump, alone, would be more than the cost of the traditional diffusion-based battery. However, for batteries several magnitudes larger, the monetary savings in separator sheet and cathode intercalation material costs can offset the cost of using a circulation pump. Typical applications of the convection battery would be plug-in hybrid electric vehicles and electric grid energy storage.

This article reports on the validation of the flow battery and includes the identification of key overpotential losses of rudimentary flow battery designs. Approaches are

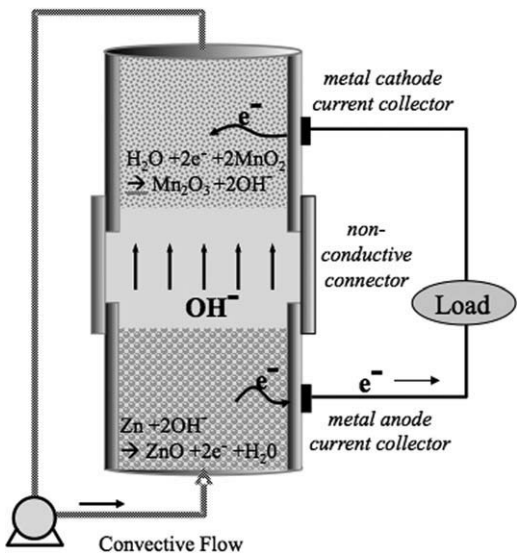

Figure 2. Schematic of a stacked electrode flow cell.

The stacked electrode flow cell uses packed-bed electrodes with tubular stainless steel current collectors separated by a nonconductive coupling.

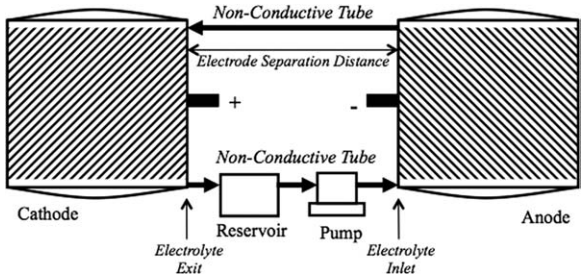

Figure 3. Schematic of a flow cell.

The flow cell is composed of separate packed-bed electrodes with stainless steel cylindrical current collectors separated by nonconductive tubing.

demonstrated that overcome the major overpotentials of the rudimentary designs. The purpose of this work is to evaluate the impact of materials and architectures of this novel flow battery on performance. At this point in research, battery cycling studies are not needed and were not performed.

Experimental

Two types of flow cell designs were used in these validation studies. One design (Figure 3) is ideal for evaluating relatively large electrode separation distances, whereas the other design (Figure 2) is a more practical flow battery design. Both of these designs incorporate packed beds of electrochemically active materials as the anode and cathode, and both designs use tubular stainless steel current collectors at the anode and cathode.

Electrode separation distance

Figure 3 is a schematic of the flow cell design in which separation distances between 2.5 cm and 43 cm were evaluated. The anode and cathode assemblies are separate stainless steel cylinders, each with a precision-machined stainless steel piston equipped with an o-ring seal that allows for material compression and current collection. Each electrode assembly has an electrolyte inlet through the wall of the cylinder near the base and an electrolyte exit, which is on the opposite side of the cylinder from the inlet, near the top. This arrangement ensures that flow is directed through the entire packed-bed electrode. Nylon hose barbs were attached to inlet and exit ports of the anode and cathode assemblies to facilitate the use of laboratory tubing connections between the electrodes. Different lengths of Masterflex Norprene peristaltic pump hose (Cole-Parmer) were used to separate the anode and cathode assemblies.

In the evaluation of electrode separation distance effects on the flow battery, granular zinc (99.8%, 110–50 mesh, ACS reagent grade; Sigma Aldrich) was used as the anode active material, while two different cathode compositions were used. The first cathode composition consisted of cathode materials harvested from a Duracell Procell alkaline battery. This material is believed to contain binder, which on compression was hypothesized to hinder flow through material, and therefore, this material was combined with stainless steel wool (Briwax Online) and stainless steel shot (0.4 mm; Pellets, LLC) to increase bed permeability. The second cathode composition consisted of 25 wt % manganese(IV) oxide (60–230 mesh, $\geq$99%; Sigma Aldrich) as active material and 75 wt % graphite (approximately 0.2 mm; Sigma Aldrich) as a bed-conductivity enhancer. A 2 M potassium hydroxide ($\geq$90%, reagent grade; Sigma Aldrich) in distilled water solution was used as the electrolyte.

Cell assembly began by loading glass wool into the hose barbs to prevent materials from being carried away by electrolyte flow. The electrode materials were then mixed and loaded into their respective cylinders, and then pistons were inserted into the cylinders. Masses of approximately 5.6 kg were loaded onto each piston to ensure packed-bed compaction. Circulation tubes were then connected to electrode assemblies, and then feed and discharge lines were inserted into the electrolyte reservoir. The feed line was then inserted and secured into a Masterflex Easy Load II L/S pump head driven by a Masterflex console pump drive, and then electrolyte flow was initiated.

The flow batteries with 2.5-, 13-, 23-, 33-, and 43-cm separation distances were each subjected to a 550-Ω external load, and cell potentials were recorded as a function of time using a personal computer equipped with a National Instruments PCI-6024E data acquisition card connected to a National Instruments SCB-68 shielded I/O connector block. A custom LabVIEW virtual instrument (VI) file served as the graphical user interface for data acquisition. Once leads from the connector block were connected to the electrode pistons, data acquisition could be initiated. Once started, the LabVIEW VI simultaneously sends a signal to close the external circuit (through use of a relay) and begins to record data. Once the user-defined discharge time elapses, the VI opens the external circuit and stops data acquisition.

Electrolyte flow vs. no flow

Electrolyte flow studies were conducted in a stacked packed-bed arrangement as shown in Figure 2. Sections of 2.5-cm long and 1.25-cm outside diameter stainless steel tube were used as the anode and cathode current collectors. These anode and cathode sections were joined with a custom machined high-density polyethylene (HDPE) coupling equipped with o-ring seals to form a liquid-tight seal around the inserted electrode current collectors. A nonconductive HDPE top piece was custom machined to act as both a piston for transferring pressure to packed beds and as an electrolyte outlet, as it was tapped and fitted with a nylon hose barb. An HDPE bottom piece was machined similar to the coupling with an o-ring seal to seal around the inserted anode current collector and tapped and fitted with a nylon hose barb to provide an electrolyte inlet. Similar to the electrode separation distance experiments, granular zinc was used as the anode material in the electrolyte flow study. A 30 wt % manganese(IV) oxide, 35 wt % graphite, and 35 wt % ALL-CRAFT 4K-activated carbon (US Patent Publication 2008-0207442) mixture was used as the cathode mixture. Electrolyte mixtures of 2, 3, and 4 M potassium hydroxide in distilled water were used in these studies.

Cell assembly began by placing a 1.25-cm diameter piece of Fisherbrand P8 filter paper (Fischer Scientific) inside the HDPE bottom cell piece, beyond the o-ring seal until is rested against the bottom. The stainless steel anode current

collector was then rotated and pressed into the bottom HDPE piece by hand until visual inspection revealed that it was completely inserted. Granular zinc was then added into the anode current collector and compacted by hand using a stainless steel rod. Once anode collector was full of zinc, three 1.25-cm diameter pieces of filter paper were inserted into one side of the HDPE coupling. Care was taken to make sure that filter paper remained uncreased and that it was seated against the center lip inside the coupling. The side of the coupling that the filter paper was inserted into was then rotated and pressed over the full anode collector until it was firmly seated over the collector. The cathode current collector was then inserted into the other side of the coupling, and visual inspection was used to make sure that it was firmly seated on the center lip of the coupling. The cathode mixture was then added in small increments with hand compression following each added increment. Once all of the cathode mixture was added, the outlet at the tip of the HDPE piston was covered with two wetted 0.95-cm diameter pieces of filter paper to prevent loss of active material, and then the piston was inserted into the cathode current collector to complete the cell assembly. The cell was then loaded into a small hydraulic press, and Masterflex peristaltic pump hose was used to connect the electrolyte inlet and outlet to the electrolyte reservoir. The feed line was then inserted into the pump head and electrolyte flow was initiated.

Flow cells using each electrolyte concentration were subjected to a 550-Ω external load for 20 min with electrolyte flow, then the flow was ceased for 20 min, and then flow was resumed for 20 min. Also, 30-min discharges (550 Ω) with and without 2 M potassium hydroxide flow were conducted to directly compare differences in their voltage profiles. The same data acquisition system discussed previously was used for these experiments.

Ion exchange material

A stacked packed-bed cell similar to that used in the electrolyte flow study (Figure 2) was used to evaluate the effects of the addition of an ion exchange resin between the anode and the cathode. The only difference to the cell used for this study is that an additional 2.5-cm long and 1.25-cm diameter stainless steel cylinder and an additional HDPE coupling were used to accommodate the addition of the ion exchange resin. Granular zinc was used as the anode material, and a mixture of 30 wt % manganese(IV) oxide, 35 wt % graphite, and 35 wt % ALL-CRAFT 4K-activated carbon was used for the cathode mixture. A 2 M potassium hydroxide in distilled water solution was used as the electrolyte in this study. All assembly steps remained the same as electrolyte flow study, except for the addition of a third middle section that was hand packed full of Amberlyst A-26(OH) (Sigma Aldrich), which is a strong basic ion exchange resin. Again, the cells were subjected to a 550-Ω external load, and a personal computer and National Instruments hardware and software were used for data acquisition.

Results and Discussion

Electrolyte flow vs. no flow

Three electrolyte concentrations (2, 3, and 4 M KOH) were used in an alternating flow:no-flow:flow scheme to determine the magnitude of overpotentials associated with electrolyte flow and to understand how the cell rebounds after electrolyte flow is restored. It was hypothesized that higher concentrated electrolytes would benefit by having a larger number of anions locally present at electrodes when electrolyte flow was ceased.

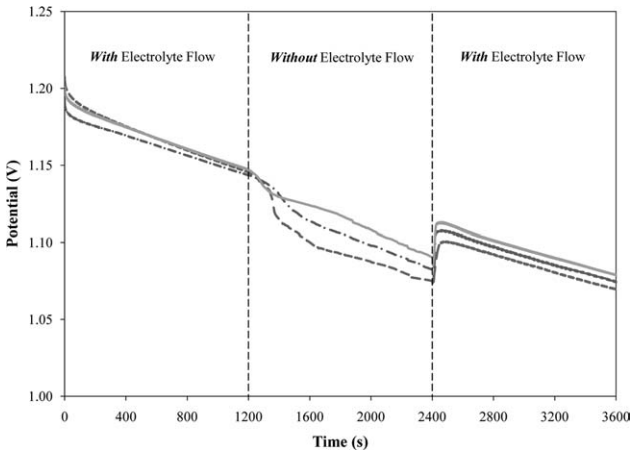

Figure 4. Electrolyte flow effects on stacked flow cell potential under a 550-Ω load at three different electrolyte concentrations [4 M KOH (solid line), 3 M KOH (dash dotted line), and 2 M KOH (dashed line)].

Figure 4 illustrates the impact of stopping electrolyte flow and how the differences in electrolyte molarity affect flow battery performance. After stopping electrolyte flow, the voltage profiles remain unchanged for a small amount of time before an increase in the rate of voltage loss occurs. The increase in the rate of voltage loss is due to the continuous consumption of OH^- (reactive ion) ions locally present in the anode when the instance flow is stopped and also to an accumulation of OH^- ions in the cathode as they are produced. The accumulation of OH^- ions in the cathode has a negative effect on the cathode reaction kinetics, which leads to a negative effect on the cell potential. After restarting electrolyte flow, the cell voltage rebounds back to a value similar to that before electrolyte flow was turned off. This occurs because of the replenishment of OH^- ions in the anode and the removal of the accumulated OH^- ions in the cathode allow the electrochemical reactions to proceed with more favorable kinetics, and therefore a higher cell potential.

It is also evident from Figure 4 that higher concentration electrolytes allow the flow cell to operate at higher voltages for longer periods of time without electrolyte flow. This is due to higher concentration electrolytes providing larger reservoirs of reactive OH^- ions when the time electrolyte flow is stopped. The more OH^- ions initially present in the anode will allow the flow cell to operate at a sustained voltage for a longer period of time.

A simple comparison of discharge runs with and without flow of a 2 M potassium hydroxide is shown in Figure 5. Despite a low current draw (550 Ω) from the flow cell, Figure 5 shows that there is about 48 mV difference, after 30 min of discharge, between discharge runs with and without electrolyte flow. A higher discharge rate would be suspected to increase this voltage separation at the 30-min mark.

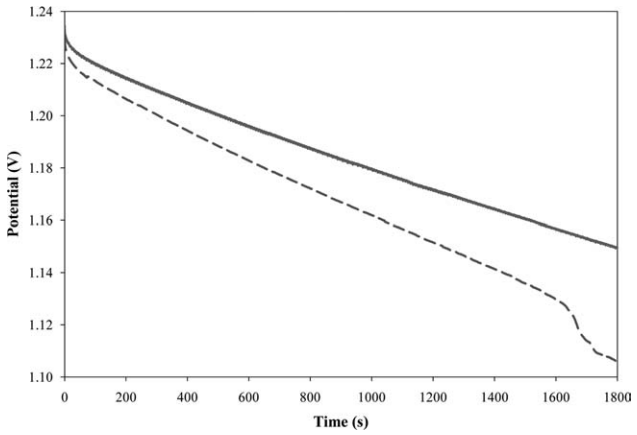

Figure 5. Thirty-minute discharge at 550-Ω load with (solid) and without electrolyte flow (dashed) using 2 M KOH electrolyte.

Electrode separation distance

A goal of the convection battery design is to separate the electrodes by a sufficiently large distance so as to eliminate dendrite modes of battery failure. Figure 6 summarizes the impact of separation distance between the electrodes on the operating voltage of the cell. Shorter separation distances exhibited higher operating voltages. The hypothesis, which explains this behavior, is that the flow of electrolyte provides the desired transfer of the OH^- anion for the zinc-alkaline battery; however, the flow introduces a new need for counter diffusion of the K^+ counterion. The need for counterion diffusion and associated effects would only become stronger with increased separation distances between the anode and the cathode as the counterions would need to diffuse a greater distance against convective electrolyte flow, and this is confirmed by the trend shown in Figure 6.

Figure 7A illustrates the mass transfer mechanism associated with a diffusion-based battery where the electrolyte is stagnant, so that the K^+ ions are nonmobile and able to stabilize the concentration-driven (as a result of electrochemical reaction) diffusion of the OH^- ions. Figure 7B depicts the hypothesized mechanism occurring in a flow cell, in which the electrolyte flows from cathode to anode. Immediately leaving the cathode, the electrolyte is unstable due to a local excess of OH^- ions. To stabilize the transport of OH^- ions, K^+ ions must counter diffuse to balance the charge of the excess OH^- ions. This situation creates a transport-based overpotential. It is hypothesized that this overpotential can be reduced by the use of a cationic ion exchange resin between the cathode and the anode that would provide stability to the excess OH^- ions being transported.

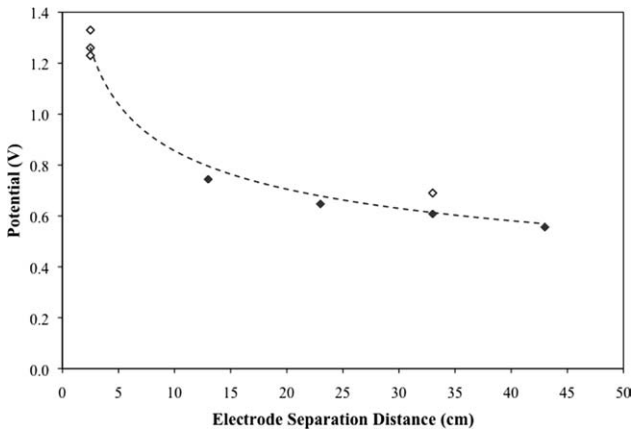

Figure 6. Electrode separation distance effects on flow cell–closed circuit potential.

Hollow diamonds indicate flow cell with harvested cathode from Duracell Procell alkaline battery mixed with stainless steel wool and shot, and solid diamonds indicate flow cell with cathode composition of 25 wt % manganese(IV) oxide and 75 wt % graphite.

Ion exchange material

A hypothesized approach to overcome the counterion counter-diffusion problem when flowing from a cathode to anode is to use an ion exchange resin that has a fixed cationic charge to provide stability for the transport of excess anions in solution. Figure 7C illustrates this proposed

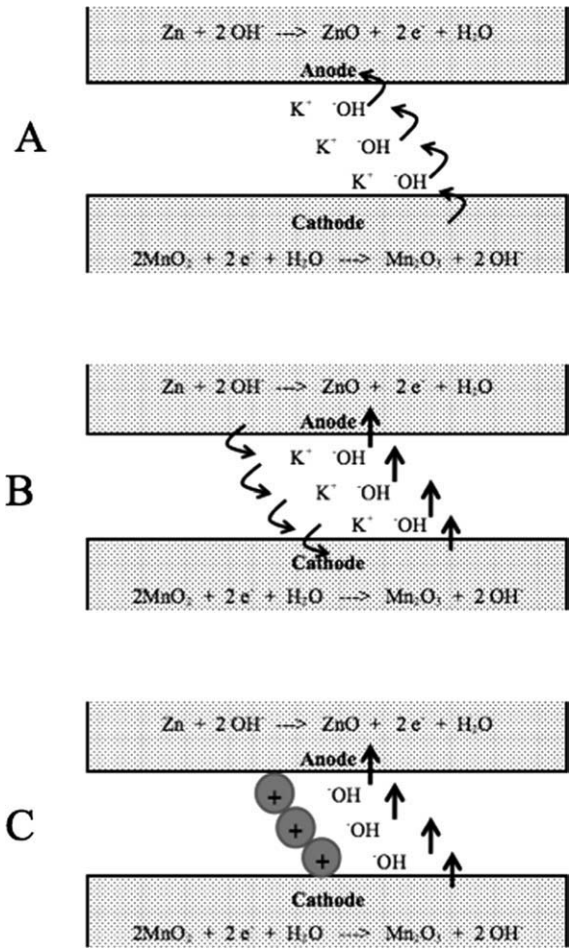

Figure 7. Illustration of mass transfer of hydroxide ions with three different approaches.

(A) Sandwich configuration (diffusion) cell, (B) convection battery where the material of the spacer does not interact with the ions, and (C) convection battery with nonconductive cation exchange material between the electrodes. The cation exchange material improves performance by reducing the need for counterion counter diffusion.

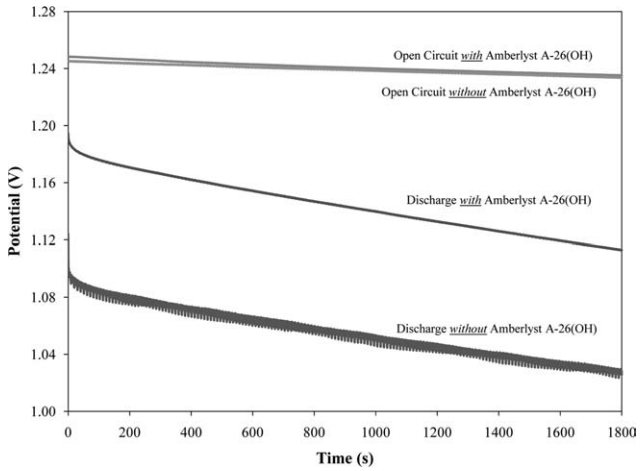

Figure 8. Comparison of flow cell performance under 550-Ω load with and without Amberlyst A-26(OH) anionic ion exchange material between electrodes.

mechanism by using an ion exchange resin with a fixed cationic charge to stabilize the excess OH^- being transported between the cathode and the anode.

With electrolyte flowing from anode to cathode, an improvement in performance (Figure 8) was attained with the addition of Amberlyst A-26(OH) anionic ion exchange resin between the electrodes (fixed anionic charge to stabilize a local excess of K^+ ions being transported from anode to cathode). Amberlyst A-26(OH) reduced the overpotential by about 80 mV and kept the useable potential well above 1 V. This improvement indicates a more efficient (less overpotential loss) use of the active materials by allowing the cell to operate at higher voltages for a longer period of time.

Figure 7C illustrates the interesting concept of sustaining an electrolyte flow in which the electrolyte has a net negative charge. This configuration illustrates the approach to literally pump anions (without counterions) from the cathode to the anode. As summarized by the anodic half-reaction for this zinc-alkaline battery (Eq. 1), the hydroxide anions are the reactive ion and the potassium cations are only necessary to stabilize the hydroxide ions in solution.

$$Zn + 2OH^- \rightarrow ZnO + H_2O + 2e^- \quad (1)$$

As the flowing electrolyte leaves the anode it has a net positive charge, which represent a high-energy and unstable state that would ultimately limit the ability to pump anions from the cathode to the anode. The energy state of this fluid leaving the anode must be reduced for the flow battery to reach its potential. Figure 9 illustrates a configuration that would reduce the energy state through use of a second bed of ion exchange resin.

By the use of two ion exchange resin sections between three electrodes, a net anion flow from the first cathode to the anode is balanced by a net cation flow from the anode to the second cathode. The electrolyte leaving the second cathode has zero net charge, and the electrolyte halfway through the depth of the anode will have a net zero charge.

These results are with an off-the-shelf ion exchange resin consistent with what is used in ion exchange chromatography. Ion exchange materials specifically designed and fabricated for this application would be expected to improve performance.

The traditional diffusion overpotential loss term is more accurately described as mass transfer overpotential for the system of Figure 9. The mass transfer overpotential has contributions from ion convection, counterion counter diffusion, and boundary layer diffusion from the flowing electrolyte to the surfaces of the electrodes.

Ion convection overpotential losses can be made negligible by increasing the electrolyte flow rate. Electrolyte flow rates for these studies varied between 400 and 850 times what was required by stoichiometry of the electrochemical reactions. As the electrolyte flows through the packed bed, it will become depleted in the reactive ion. Thinner electrodes will also decrease these losses.

Counterion counter-diffusion overpotential losses can be reduced by the development of ion exchange materials that are able to effectively stabilize ions being transported between the electrodes. Equally important will be the use of ion exchange materials in the packed beds. The maximum power output per cross-sectional area (perpendicular to flow) will be limited by the performance of this ion exchange media. When operating at high-power output where the capabilities of the ion exchange material are reached, it is expected that the voltage of the cell vs. the electrolyte flow rate will have a maximum. At lower flow rates, the convection of the ions is not adequate to meet power requirements, whereas at higher flow rates, counterion counter diffusion will be required as the capacity of the ion exchange material is exceeded.

Boundary layer diffusion overpotential losses can be reduced by increasing the boundary layer surface area and by increasing the specific active surface area of the particles. Smaller particles will decrease this overpotential, but only at the expense of increasing pressure drops for flow through the packed beds. There will always be an optimal permeability, which can be related to particle size distributions, that balances boundary layer diffusion overpotential with pressure drop for flow through the bed. Ultrahigh surface area mesoporous carbons (>3000 m^2/g) will reduce these diffusion overpotential losses. These same carbons may also provide ion exchange capacity in the packed beds.

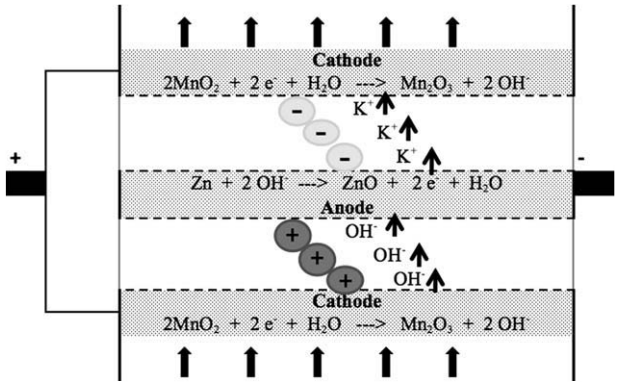

Figure 9. Illustration of flow cell electrode configuration designed to stabilize the flow of electrolyte with net charges.

The ability to which these three overpotential losses can be overcome to achieve higher levels of charge flux for pumping anions/cations between electrodes is an unexplored area of science with immediate application. The flow battery design overcomes the traditional battery design paradigm in which increased power in a battery has been at the expense of decreasing the energy density and increasing the battery costs (more membrane area and thinner electrodes). When the ability to pump anions and cations between electrodes is combined with ultrahigh surface area carbons, it may be possible to create low-cost batteries that can provide 320 km of travel in electric vehicles and be charged in times comparable to the time it takes to refuel with gasoline.

Conclusions

A new type of flow battery has been validated in which all reagents and products remain as solids on the electrodes. This flow battery has the potential to gain higher energy densities than other types of flow batteries and provides an excellent platform for rechargeable lithium batteries that allow use of metallic lithium in the anode. An approach incorporating a permeable ion exchange material between electrodes was validated and is hypothesized to be a key aspect of this flow battery design to maximize the power output per area of separator between electrodes.

Acknowledgments

The authors thank the National Science Foundation (Award 0940720) and the following graduate and undergraduate coresearchers: Alex R. Hunter, Eric Leimkuehler, Eric M. Nordwald, Ashley N. Ulrich, Matt Wavada, and Matthias Young.

Literature Cited

1. Zhang SS. A review on the separators of liquid electrolyte Li-ion batteries. *J Power Sources*. 2007;164:351–364.
2. Gaines L. *Costs of Lithium-Ion Batteries for Vehicles*. Argonne, IL: Argonne National Laboratory, 2000.
3. Treptow RS. Lithium batteries: a practical application of chemical principles. *J Chem Educ*. 2003;80:1015–1020.
4. Cheng J, Luo X, Yan X, Li Z, Tang Y, Jiang H, Zhu W. Research progress in cation-pi interactions. *Sci China Ser B: Chem*. 2008;51:709–717.
5. Radford GJW, Cox J, Wills RGA, Walsh FC. Electrochemical characterization of activated carbon particles used in redox flow battery electrodes. *J Power Sources*. 2008;185:1499–1504.
6. Wang X, Wang Y, Xue F, Li J, Liu Y, Wang T, Ye F, Miao R (Inventors; University of Science and Technology Beijing, Peoples Republic of China). Integrated device of electrode tank and current collector for redox flow battery. U.S. Pat. 2008-20,108,417, 201,204,228, 20,080,530, 2009.
7. Zhang L, Cheng J, Yang Y-S, Wen Y-H, Wang X-D, Cao G-P. Study of zinc electrodes for single flow zinc/nickel battery application. *J Power Sources*. 2008;179:381–387.
8. Hazza A, Pletcher D, Wills R. A novel flow battery: a lead acid battery based on an electrolyte with soluble lead(II). I. Preliminary studies. *Phys Chem Chem Phys*. 2004;6:1773–1778.
9. Li X, Pletcher D, Walsh FC. A novel flow battery: a lead acid battery based on an electrolyte with soluble lead(II). *Electrochim Acta*. 2009;54:4688–4695.
10. Pletcher D, Wills R. A novel flow battery—a lead acid battery based on an electrolyte with soluble lead(II). *J Power Sources*. 2005;149:96–102.
11. Pan J, Sun Y, Cheng J, Wen Y, Yang Y, Wan P. Study on a new single flow acid Cu-PbO2 battery. *Electrochem Commun*. 2008;10:1226–1229.
12. Cheng J, Zhang L, Yang Y-S, Wen Y-H, Cao G-P, Wang X-D. Preliminary study of single flow zinc-nickel battery. *Electrochem Commun*. 2007;9:2639–2642.
13. Puskar M, Harris P. Reserve, flowing electrolyte, high rate lithium battery. *Proc Int Power Sources Symp*. 1986;32:331–336.
14. Hart TG (Inventor; Energy Development Associates, Inc.). Electrochemical system. U.S. Pat. 4,237,197, 1980.
15. Pan J, Ji L, Sun Y, Wan P, Cheng J, Yang Y, Fan M. Preliminary study of alkaline single flowing Zn-O_2 battery. *Electrochem Commun*. 2009;11:2191–2194.
16. Zocchi A (Inventor; Squirrel Holdings Ltd.). Redox flow battery and method of operating it. U.S. Pat. 6,692,862-B1, 2004.

Manuscript received Feb. 12, 2010, and revision received July 13, 2010.